Pt adatom diffusion on strained Pt(001)

Wei Xiao, P. Alex Greaney, and D. C. Chrzan*
Department of Materials Science and Engineering, University of California, Berkeley, California 94720, USA
(Received 7 December 2003; published 9 July 2004)

The diffusion of Pt on unreconstructed, strained Pt(001) is considered. The strain dependence for the energy barrier to adatom diffusion is computed using the embedded atom method. The computations predict that for a broad range of accessible strain states, the dominant diffusion mechanism is mediated by the formation and motion of a surface crowdion. Further, the saddle-point configuration for ''simple'' hopping is predicted to extend over a number of lattice sites. The diffusion energy barriers for both exchange and hopping mechanisms depend on the size of the cell used in the calculation.

DOI: 10.1103/PhysRevB.70.033402 PACS number(s): 68.43.Jk, 61.72.Cc, 61.72.Ji

Surface diffusion has been of significant scientific interest for many years. It has been recognized that surface diffusion is the key problem in most dynamical processes on surfaces, for example, island growth and surface chemical reactions. An excellent review of this subject was presented recently by Ala-Nissila, *et al.*[1] Experimental work based on field ion microscopy (FIM) provides important information concerning surface diffusion.[2,3] In their pioneering studies of diffusion of Pt on Pt(001), Kellogg and Feibelman identified an adatom diffusion mechanism known as exchange; a mechanism by which a surface adatom displaces a substrate atom through a concerted motion of the pair.[4,5] This mechanism differs substantially from the simple hopping mechanism (Fig. 1) assumed implicitly in many studies. The concerted exchange mechanism leads to apparent hopping along $\langle 100 \rangle$ directions, and consequently leads to occupation of only every other site on the surface of the substrate, i.e., the visited sites form a $c(2\times2)$ pattern on the surface. This pattern is readily apparent in FIM experiments, and Kellogg and Feibelman established unambiguously that under typical conditions, diffusion of Pt on unreconstructed Pt(001) involves the proposed exchange mechanism.

Consider thin-film growth. If there is lattice mismatch between the substrate and the film material, the film may be strained. Subsequent growth takes place upon this strained surface, and modeling of this growth requires that one understand the role that strain plays in diffusion. Further, since the strain may affect directly energy barriers for diffusion, small strains may strongly influence adatom diffusion rates. Consequently, some effort has been expended in an effort to understand the role that strain plays in adatom diffusion.[6–8]

Theoretical studies of adatom diffusion on (001) surfaces of fcc metals have been presented in the literature. Yu and Scheffler applied density-functional theory[7] and showed that for adatom self-diffusion on strained Au (001) and Ag (001), the hopping diffusion energy barrier *increases* with increasing tensile stress and exchange diffusion energy barrier *decreases*. This prediction is similar to a recent prediction for Cu diffusing on Cu (001) in which the energy barriers were computed as a function of an imposed two-dimensional strain.[8] The most striking result of the Cu work is the discovery of a surface crowdions under shear. The discovery of surface crowdions in Cu raises the question as to whether or not surface crowdions may mediate diffusion processes on other fcc (001) surfaces, such as Pt on Pt(001).

Total-energy calculations coded within the framework of the nudged elastic band method[9] are used to compute the strain dependence of the energy barriers for two adatom diffusion processes: ''simple'' hopping and adatom exchange (see Fig. 1). For a broad range of experimentally accessible strain states, surface crowdion formation and motion is predicted to be the adatom diffusion process with the lowest-energy barrier. Further, the saddle-point configuration for simple hopping is predicted to include displacements of a large number of surface atoms. A prior calculation[10] of saddle-point energies and configurations for Pt adatom diffusion on unreconstructed Pt (001) employed unit cells too small to observe these extended saddle-point structures and thus may have overestimated the energy barrier to hopping. Finally, over a significant range of strain states, the minimum energy diffusion path for both mechanisms passes through a metastable surface crowdion configuration.

The calculations employ the embedded atom method as coded in XMD,[15] and our own implementation of the nudged elastic band method (coded as a ''wrapper'' for XMD). The Pt potential of Foiles *et al.*[11] is used in all the presented

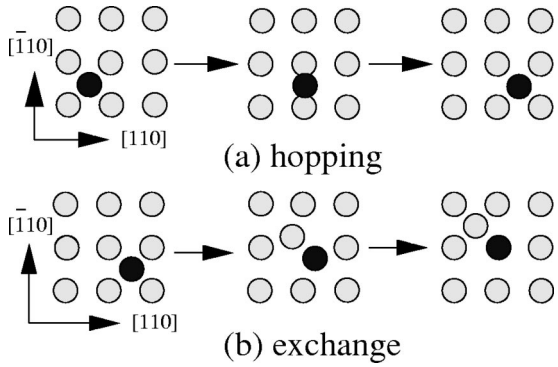

FIG. 1. Schematic of two of the adatom transport mechanisms studied in this paper. The [001] direction points out of the page. Gray atoms are initially substrate; black atoms are initially adatoms. Panel (a) depicts the simple hopping mechanism. Panel (b) depicts the exchange mechanism. The central configuration is the saddle-point configuration. Note that for exchange, the initial adatom becomes a substrate atom, and a former substrate atom becomes the new adatom.

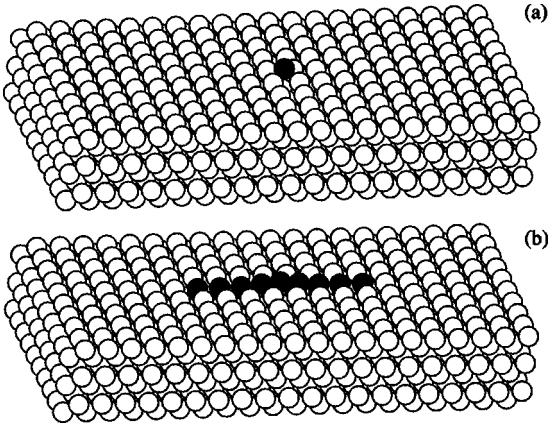

FIG. 2. The 10×20 unit cell used in many of the computations. Panel (a) is the initial configuration. Panel (b) shows saddle-point associated with simple hopping under zero applied strain. Note that the saddle-point configuration distorts the positions of four to five nearest neighbors along the $\langle 110\rangle$ normal to the hopping direction. This saddle-point structure is similar to the structure of the metastable surface crowdion that is predicted for applied compressive strains.

calculations. This potential reproduces well the elastic and structural properties of bulk Pt. The predicted surface energies are generally lower than experimental estimates.

A typical unit cell used in the calculation is shown in Fig. 2. The slab used for the majority of the calculations contains a total of 1201 atoms. This cell is large enough to minimize finite-size effects. The lateral dimensions of the cell are fixed at values appropriate for the biaxial strain state under study, and the cell relaxes completely in the direction normal to the surface. (The $[110]$ and $[\bar{1}10]$ directions of the crystal coincide with the *x* and *y* directions of the unit cell.) The nudged elastic band calculations include, typically, 15 images. The forces are relaxed to better than 0.001 eV/Å. With this set of parameters, the energy barriers are computed to an accuracy much better than 0.05 eV.

The saddle point for the exchange mechanism appears much as is expected from earlier studies.[4,5] However, the computed energy barrier is more than 0.2 eV less than the *ab initio* prediction, 0.48 eV,[10] and the measured experimental barrier of 0.47 eV.[4] The discrepancy between the embedded atom method and the experimental results is probably the result of the approximations used in computing the total energy. It is tempting to attribute the discrepancy between the predictions of *ab initio* electronic structure total-energy calculations and the present calculations also to inadequacies of the embedded atom method. However, there may be a second contribution to the discrepancy: the effects of finite size (see Fig. 3).

To investigate the effects of finite size, the energy barrier for adatom exchange was computed as a function of cell size (Fig. 3) under conditions of no imposed strain (i.e., the in-plane lattice parameters fixed at their bulk values). The energy barrier for adatom exchange is cell-size dependent. The energy barrier predicted using a 5×5 cell is 0.33 eV. (Here, the cell size is reported as $n\times m$, where *n* and *m* refer to the number of primitive cells in the $[110]$ and $[\bar{1}10]$ directions,

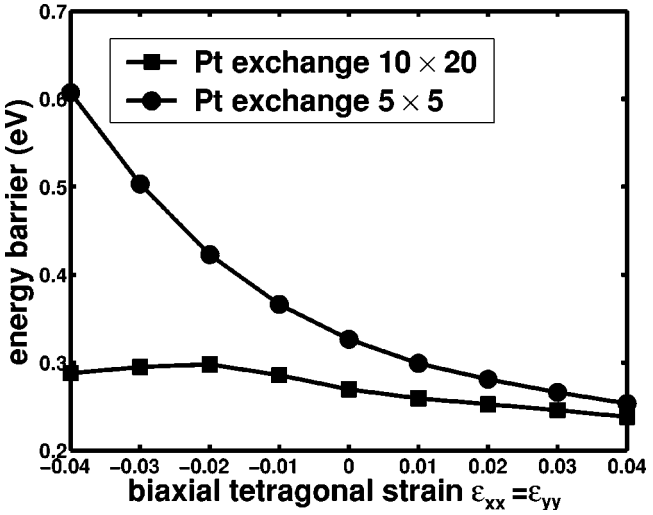

FIG. 3. Exchange mechanism energy barriers vs the size of the cell used in the computation.

with the adatom hopping in the $[110]$ direction.) The same energy barrier becomes 0.27 eV when a cell 10×20 is used for the computation. (Use of larger cells leads to no further reduction in the energy barrier.) Thus using a 5×5 cell has led to an increase in the exchange energy barrier of roughly 22%. Under compressive biaxial tetragonal strains of 4%, the energy barrier computed using the 5×5 cell is *twice* that predicted from the 10×20 cell. It should also be noted that for the larger cell considered, the exchange energy barrier is not very strongly dependent on strain.

The implications of these calculations are that the saddle point for the exchange mechanism may involve displacements of atoms over substantial distances from the adatom. The embedded atom method suggests that these displacements may extend somewhere between 5 and 10 unit cells. In contrast, the unit cells employed in Ref. 10 were only 4×4. If the extended saddle points are not an artifact of the embedded method calculations, the *ab initio* calculations may also be constrained by finite size and consequently may overestimate the zero stress adatom exchange energy barrier.[16]

While the saddle point for exchange behaves much as one expects, the saddle point for ''simple'' hopping is markedly different. During a hop along the $[110]$ direction for 10×20 cell, the adatom does not become undercoordinated by rising up from the surface. Instead, the adatom ''burrows'' into the surface, creating a line of atoms displaced along the $[\bar{1}10]$ direction. The displacements extend approximately four nearest neighbor spacings in each direction yielding a structure reminiscent of the surface crowdions identified in Ref. 8. Here, however, the surface crowdion configuration is unstable (under zero imposed strain—at higher strains, it becomes metastable). The extended nature of this saddle-point configuration for hopping suggests that prior calculations[10] of the energy barrier to adatom hopping may also be influenced by system size.

In order to examine the effects of finite size on simple hopping, the energy barrier was computed as a function of system size, and the results are displayed in Fig. 4.

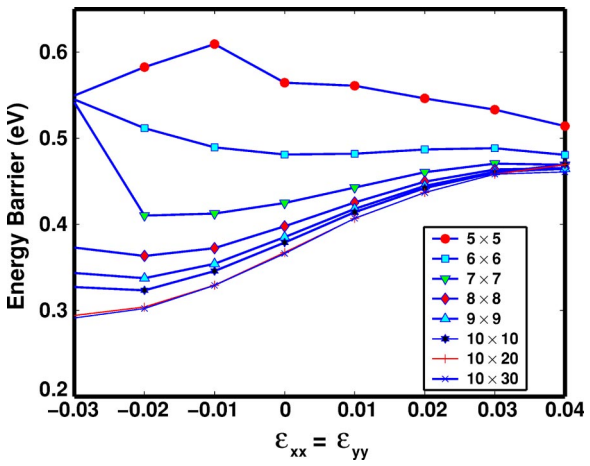

FIG. 4. (Color online) Hopping mechanism energy barriers vs the size of the cell used in the computation.

Consider, first, the zero strain state. The energy barrier for hopping in the 5×5 cell is ≈0.56 eV, whereas in the 10×30, the barrier is computed to be 0.36 eV. Thus the fact that the unit cell is ''too small'' raises the energy barrier by over 50%. The origin of this energy barrier increase can be understood simply by examining the structure of the saddle point (Fig. 2). At the energy maximum, the adatom ''squeezes'' into the row of atoms extending along the $[\bar{1}10]$ direction. For small unit cells, the density of additional atoms is too large to be accommodated with low energy. Hence the hopping mechanism reverts to the bridging saddle point that one expects intuitively.

Figure 4 also indicates the effects of a tetragonal biaxial strain on saddle-point energy for hopping. For small cells, the strain dependence of the hopping energy is the opposite of what one expects. More specifically, under compressive stresses, one expects the corrugation of the potential in which the adatom is ''hopping'' to decrease. Since the amplitude of this correlation should be linked to the energy barrier for simple hopping, when corrugation decreases with

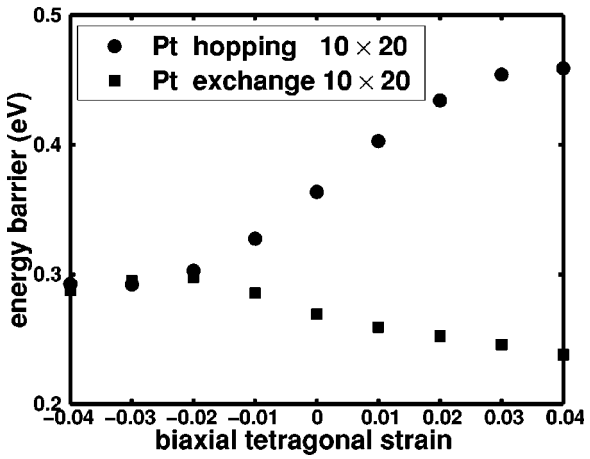

FIG. 5. Hopping and exchange energy barriers vs tetragonal biaxial strain. At a compressive strain of 2%, the energy barrier curves converge. At this point, both starting points for computation lead to the formation of a metastable surface crowdion.

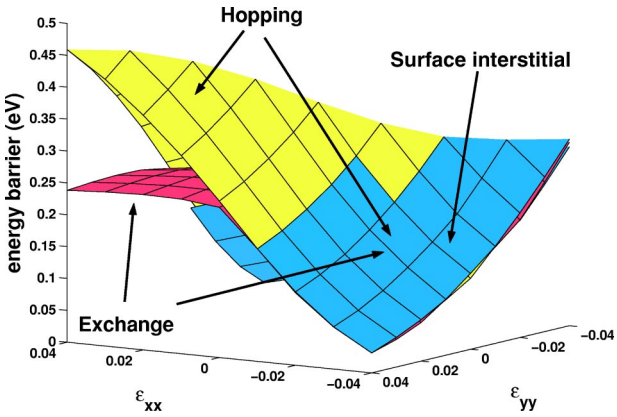

FIG. 6. (Color online) A plot of the energy barrier to hopping, exchange, and surface crowdion formation as a function of imposed strain. The exchange and hopping mechanism surface converge in the regions of strain space for which surface crowdion formation is predicted.

compression, one expects the energy barrier to hopping to decrease.[8] While for the larger cells, this is the observed behavior, the strain behavior indicated by the small cells displays the opposite trend, presumably due to constraints imposed on the saddle point by the system size.

Figure 5 compares the tetragonal biaxial strain dependence of the hopping and exchange energy barriers. The most striking feature of this plot is that at a compressive strain near -2%, the energy barriers for hopping (via the extended saddle-point configuration) and exchange converge and, in fact, become the saddle-point energy associated with the formation of a metastable surface crowdion. In fact, the

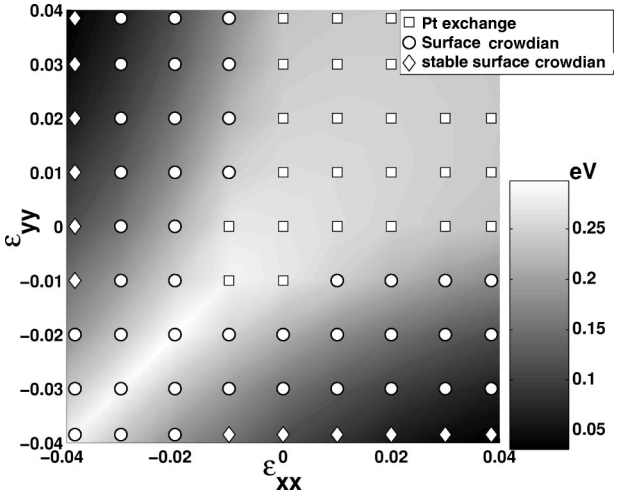

FIG. 7. Diffusion mechanism map predicted for Pt adatom diffusion on Pt (001). The plot indicates, as a function of strain state, which of the investigated mechanisms has the lowest-energy barrier. At the points labeled exchange the energy barrier to simple adatom exchange is the lowest of those investigated. The points labeled surface crowdion correspond to those for which creation of a metastable surface crowdion has the smallest energy barrier. The points labeled stable surface crowdion are those points for which a surface crowdion forms, and lowers the energy of the surface relative to the energy of the surface and an adatom.

embedded atom method predicts that there is a broad range of biaxial strain states for which the energy barrier to surface crowdion formation is the lowest for the considered adatom processes (Fig. 6). It is significant that the surface crowdion is expected for pure shear strains as small as 1% (Fig. 7). Such shear strains should be obtained relatively easily using epitaxial growth techniques and suitable substrates. Further, it is interesting to note that the formation of the crowdion. here breaks symmetry, in striking contrast to the predictions for Cu (001).

Of course, it is well known that clean Pt(001) reconstructs.[12–14] The present analysis applies only to unreconstructed Pt (001), such as that prepared and observed within the field ion microscope. (Since the reconstruction leads to a net increase in the areal atom density, it is likely that diffusion is involved in creating the reconstruction. In this case one can imagine circumstances under which the unreconstructed surface is kinetically stabilized. Alternatively, strains intrinsic to the sharp tip geometry might suppress the reconstruction.) For surface of bulk samples, the present set of potentials predict that the unreconstructed surface is at least metastable. Further, it is only for extreme shear strains that the surface crowdion becomes absolutely stable, i.e., the surface crowdion formation energy is negative (Fig. 7). (It is tempting to relate this region of absolute stability of the surface crowdion to stability of the reconstructed surface. However, the extent of this study does not allow one to draw such conclusions.) Consequently, it may be possible to observe the surface crowdions predicted here on the metastable unreconstructed surface.

The authors acknowledge the financial support of the National Science Foundation under Grant No. EEC-0085569 and computational support from the Metals Program, Materials Sciences Division, Lawrence Berkeley National Laboratories.

*Electronic address: dcchrzan@socrates.berkeley.edu

[1] T. Ala-Nissila, R. Ferrando, and S.C. Ying, Adv. Phys. **51**, 949 (2002).
[2] G. Kellogg, Surf. Sci. Rep. **21**, 1 (1994).
[3] T.T. Tsong, Rep. Prog. Phys. **51**, 759 (1988).
[4] G.L. Kellogg and P.J. Feibelman, Phys. Rev. Lett. **64**, 3143 (1990).
[5] P.J. Feibelman, Phys. Rev. Lett. **65**, 729 (1990).
[6] M. Schroeder and D.E. Wolf, Surf. Sci. **375**, 129 (1997).
[7] B.D. Yu and M. Scheffler, Phys. Rev. B **56**, 15 569 (1997).
[8] W. Xiao, P.A. Greaney, and D.C. Chrzan, Phys. Rev. Lett. **90**, 156102 (2003).
[9] H. Jónsson, G. Mills, and K.W. Jacobsen, in *Classical and Quantum Dynamics in Condensed Phase Simulations*, edited by B.J. Berne, G. Ciccotti, and D.F. Coker (World Scientific, Singapore, 1998), p. 385.
[10] P.J. Feibelman, Phys. Rev. B **64**, 125403 (2001).
[11] S.M. Foiles, M.I. Baskes, and M.S. Daw, Phys. Rev. B **33**, 7983 (1986).
[12] Q.J. Gao and T.T. Tsong, Phys. Rev. B **36**, 2547 (1987).
[13] K. Heinz, E. Lang, K. Strauss, and K. Muller, Surf. Sci. **120**, L401 (1982).
[14] M.A. van Hove, R.J. Koestner, P.C. Stair, J.P. Biberian, L.L. Kesmodel, I. Bartos, and G.A. Somorjai, Surf. Sci. **103**, 189 (1981).
[15] Jon Rifkin, University of Connecticut, http://www.ims.uconn.edu/centers/simul
[16] Our present implementation of the EAM code will not allow us to examine cells smaller than 5×5.